

Supporting Information for

Improving the retrieval of carbon-based phytoplankton biomass from satellite ocean colour observations

Marco Bellacicco^{1,2*}, Jaime Pitarch², Emanuele Organelli², Victor Martinez-Vicente³, Gianluca Volpe² and Salvatore Marullo^{1,2}

¹ Climate Modelling Laboratory, Italian National Agency for New Technologies, Energy and Sustainable Economic Development (ENEA), Via E. Fermi 45, 00044 Frascati, Italy; marco.bellacicco@enea.it (M.B.); salvatore.marullo@enea.it (S.M.)

² Consiglio Nazionale delle Ricerche (CNR), Istituto di Scienze del Mare (ISMAR), Via Fosso del Cavaliere, 100 Rome, Italy; Jaime.PitarchPortero@artov.ismar.cnr.it (J.P.); emanuele.organelli@artov.ismar.cnr.it (E.O.); gianluca.volpe@cnr.it (G.V.)

³ Plymouth Marine Laboratory (PML), Prospect Place, The Hoe, Plymouth PL1 3DH, UK; vmv@pml.ac.uk

* Correspondence: marco.bellacicco@enea.it

Contents of this file:

Figure S1 shows the scheme of the algorithm here developed.

Table S1 contains the basic statistics of the validation analysis for all the matchup with \log_{10} transformed data.

Figures S2 to S13 are the global monthly climatologies of b_{bp}^k (a), $1-\sigma$ uncertainty (b), significance S (c) and C_{phyto} (d). Note that the $1-\sigma$ uncertainty gives an estimate of uncertainty for each b_{bp}^k pixel computation. The significance S is obtained after application of t-Student Test between daily Chl- b_{bp} data at pixel scale; this can help to understand the robustness of each single fit at pixel-scale. The C_{phyto} maps are global mean monthly climatological maps obtained by the application of Eq. 3 into the manuscript to monthly climatological b_{bp} maps.

Figures S14 show the global mean and standard deviation b_{bp}^k maps.

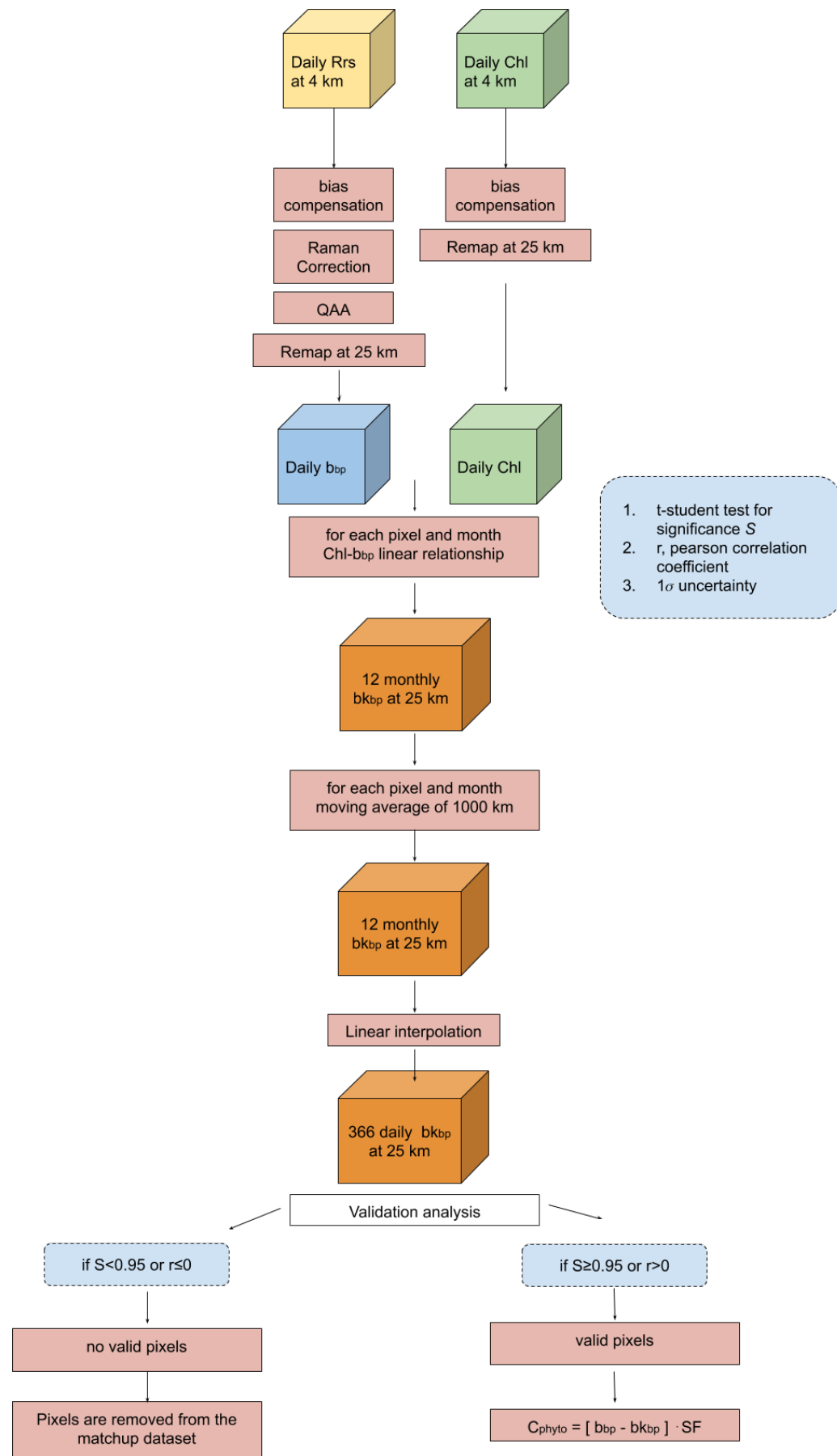


Figure S1. Scheme of the algorithm here developed. Note that bb_{bp} is at 443nm.

Table S1. Statistics for each single approach using untransformed and \log_{10} transformed data ($N=396$). δ is the bias; σ_Δ is the standard deviation of the difference and ∇ is the relative percentage bias. In bold the best values.

	\log_{10} transformed data					
	This Study	Bel18	Gra15	Beh05	Bre12	MV17
δ	-0.06	-0.02	0.33	0.26	0.13	0.37
σ_Δ	0.37	0.41	0.27	0.28	0.32	0.29
$\nabla(\%)$	0.17	5.13	44.60	36.19	21.94	48.29

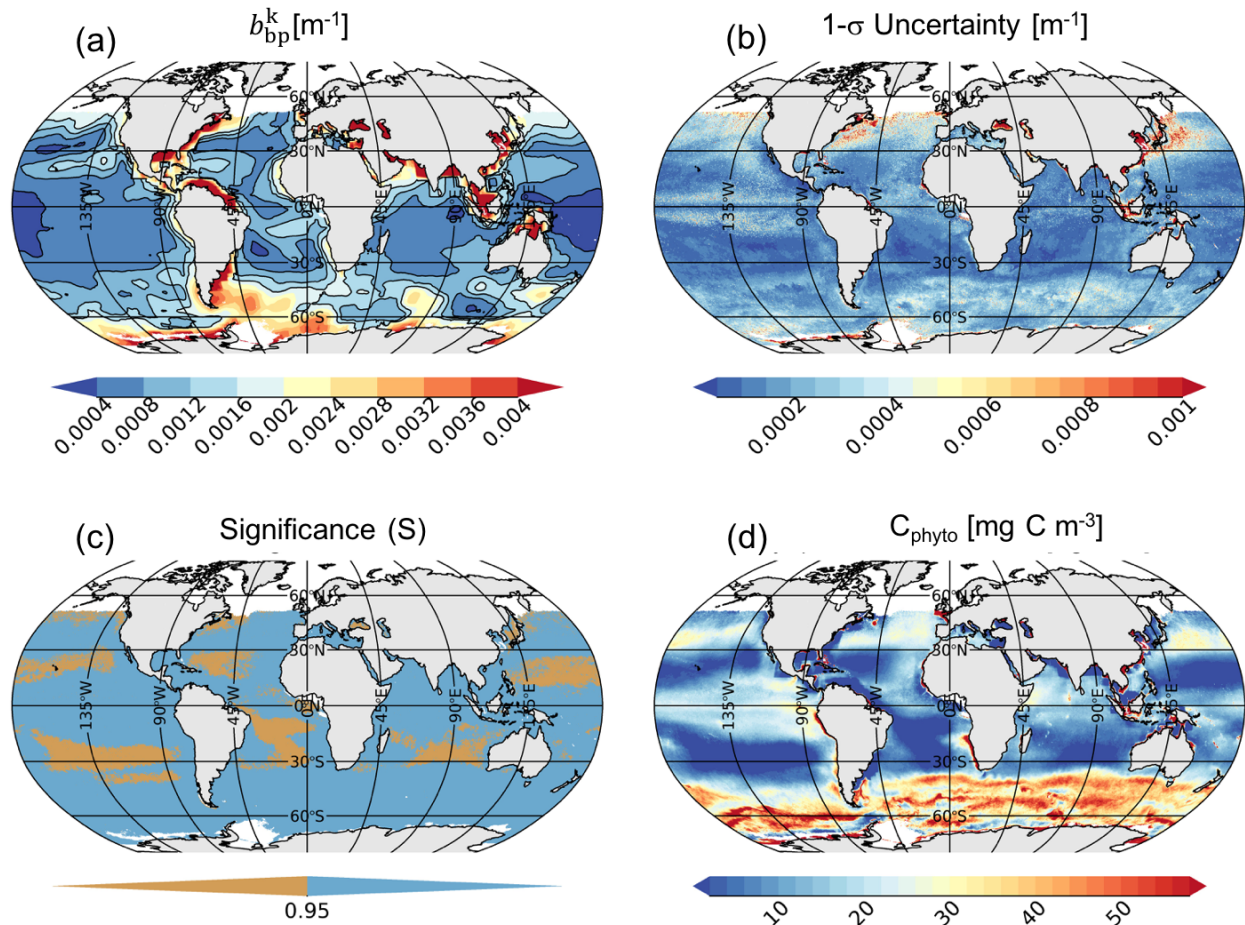


Figure S2. January global mean climatological of b_{bp}^k (a), 1- σ uncertainty (b), significance S (c) and C_{phyto} (d).

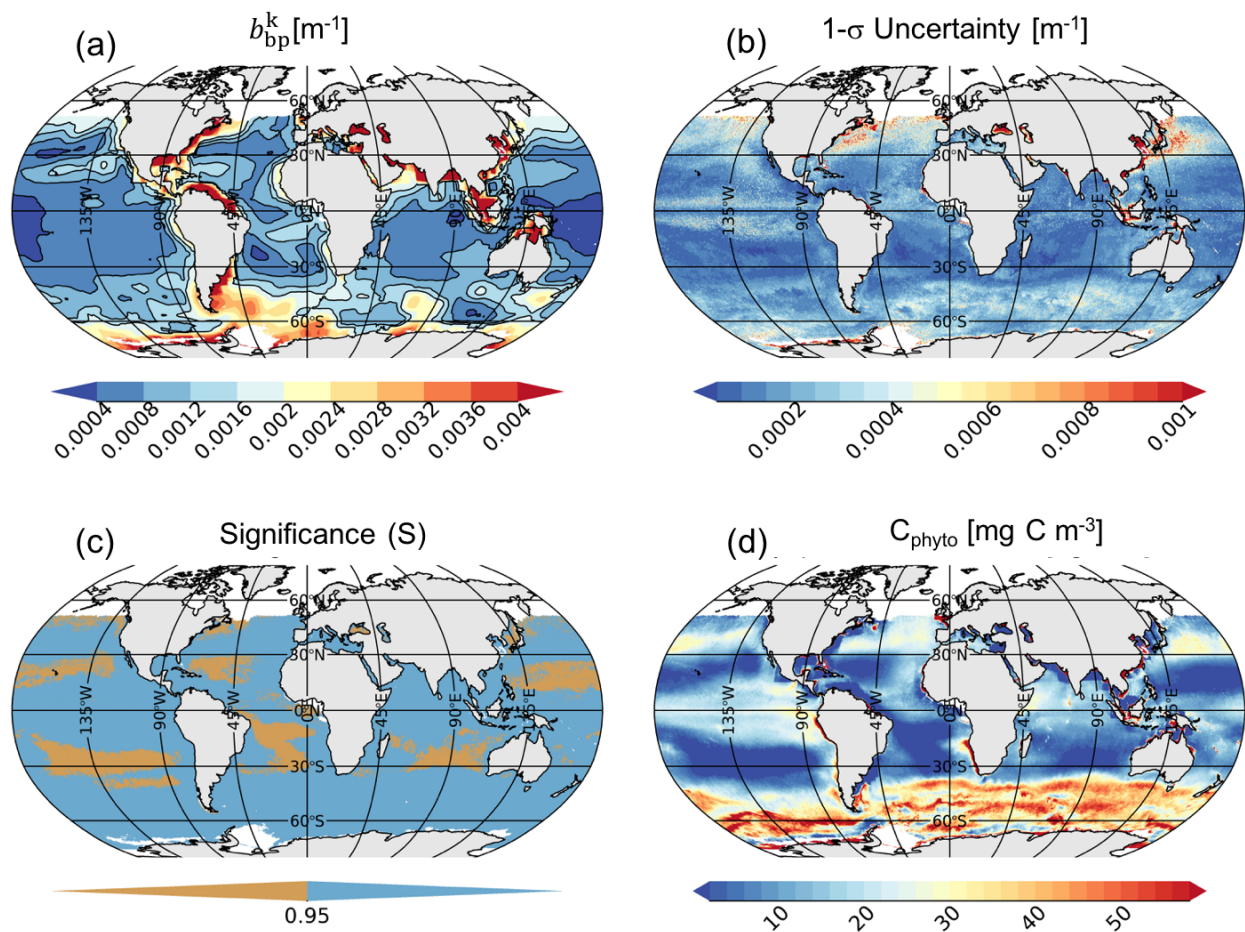


Figure S3. February global mean climatological of b_{bp}^k (a), 1- σ uncertainty (b), significance S (c) and C_{phyto} (d).

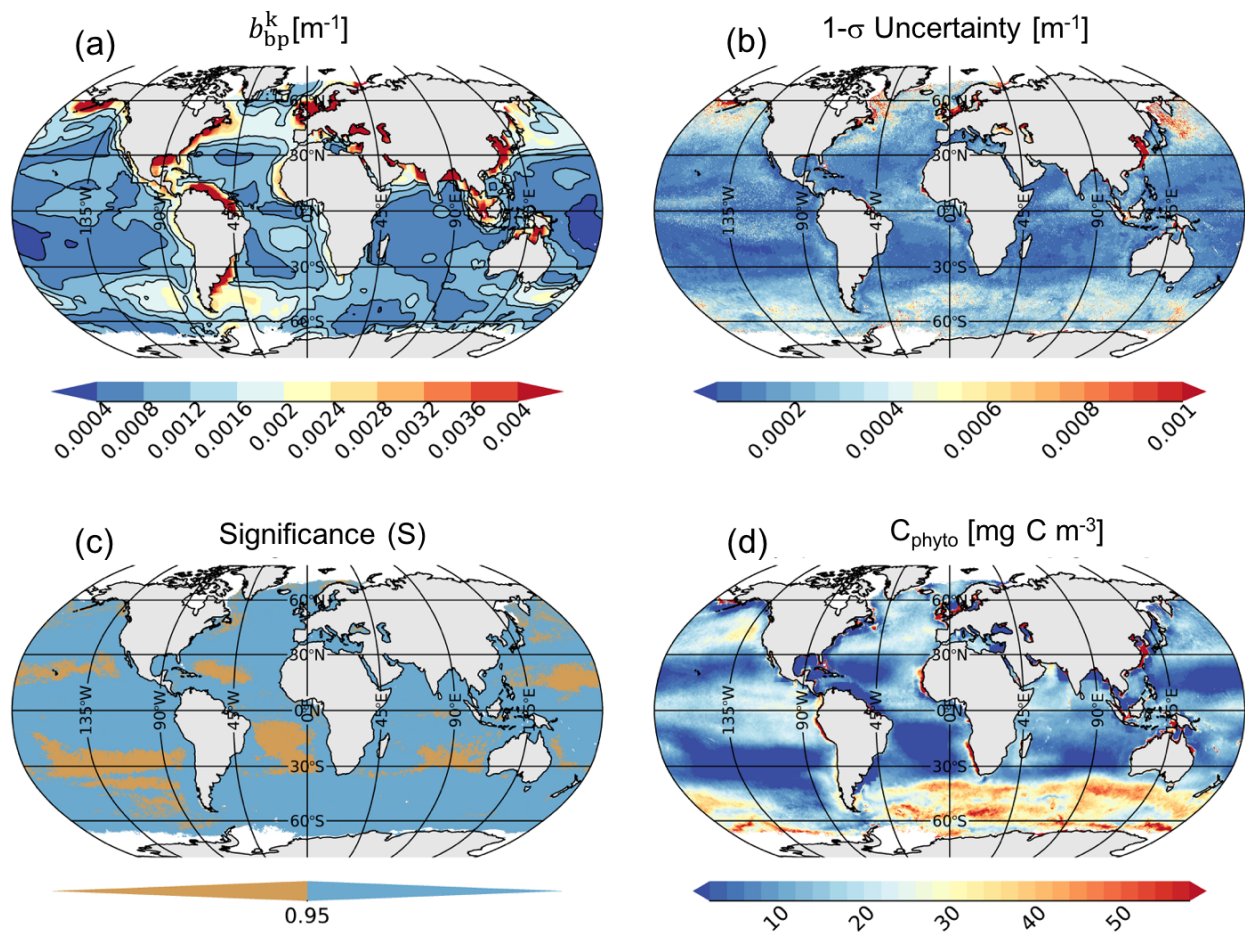


Figure S4. March global mean climatological of b_{bp}^k (a), 1- σ uncertainty (b), significance S (c) and C_{phyto} (d).

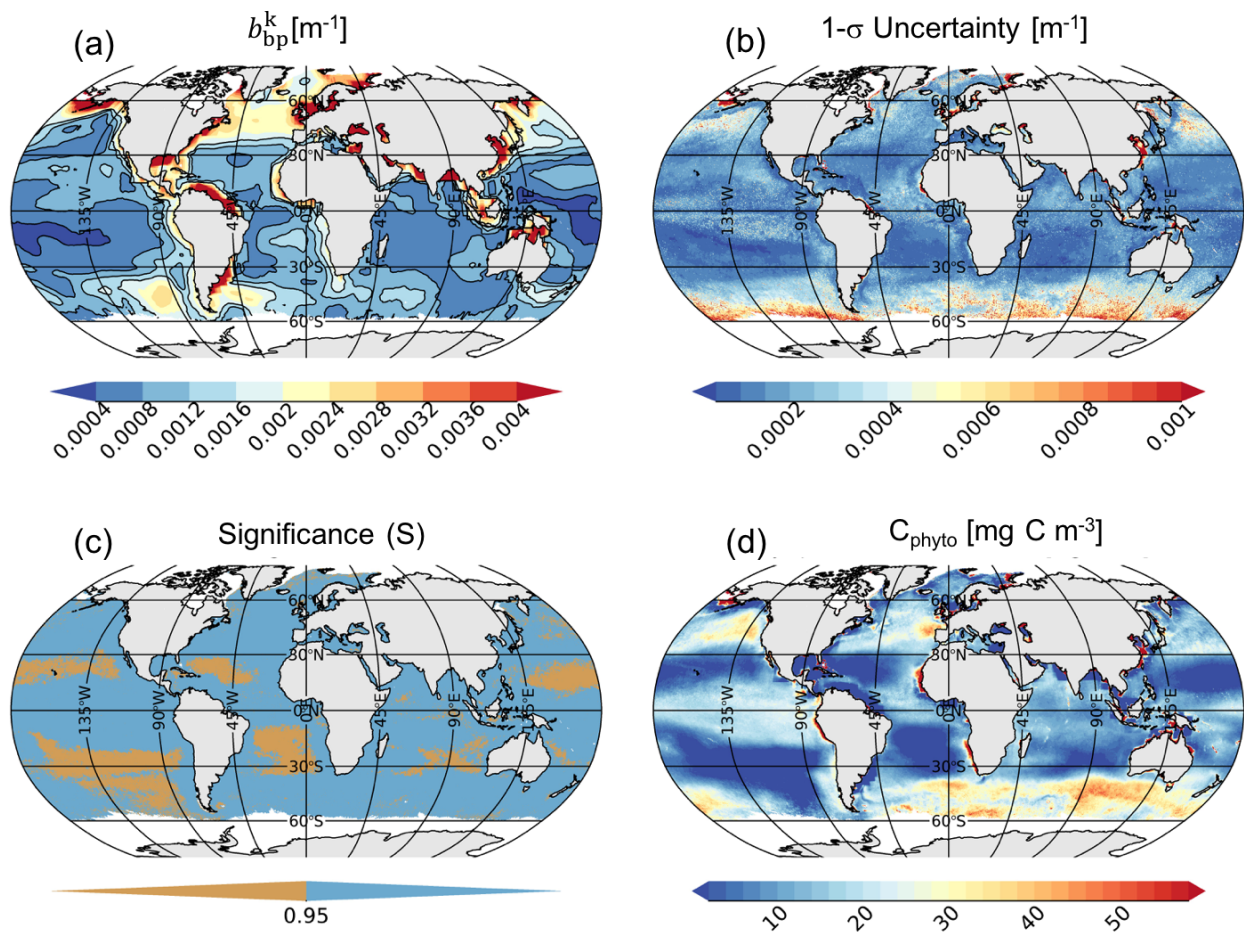


Figure S5. April global mean climatological of b_{bp}^k (a), 1- σ uncertainty (b), significance S (c) and C_{phyto} (d).

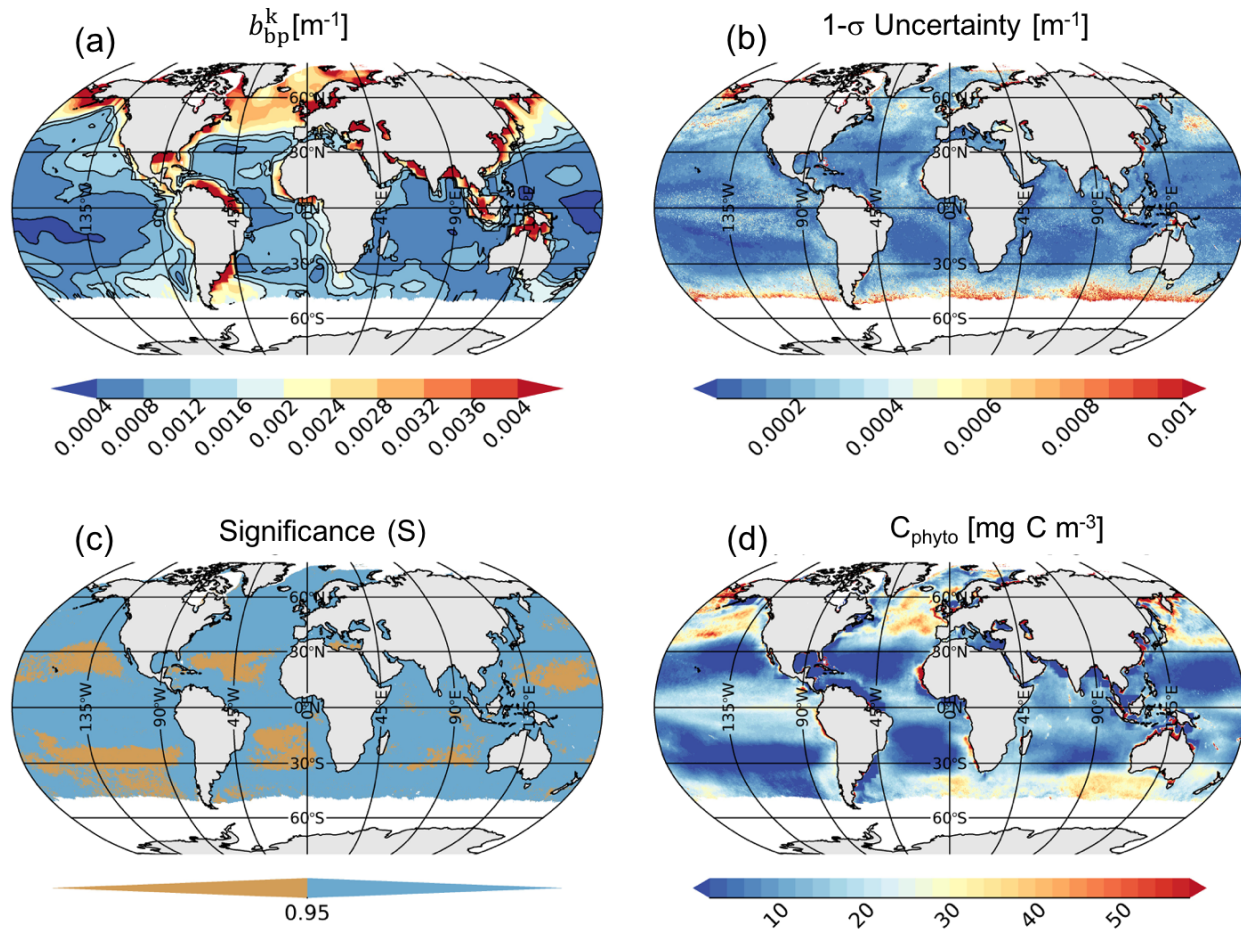


Figure S6. May global mean climatological of b_{bp}^k (a), 1- σ uncertainty (b), significance S (c) and C_{phyto} (d).

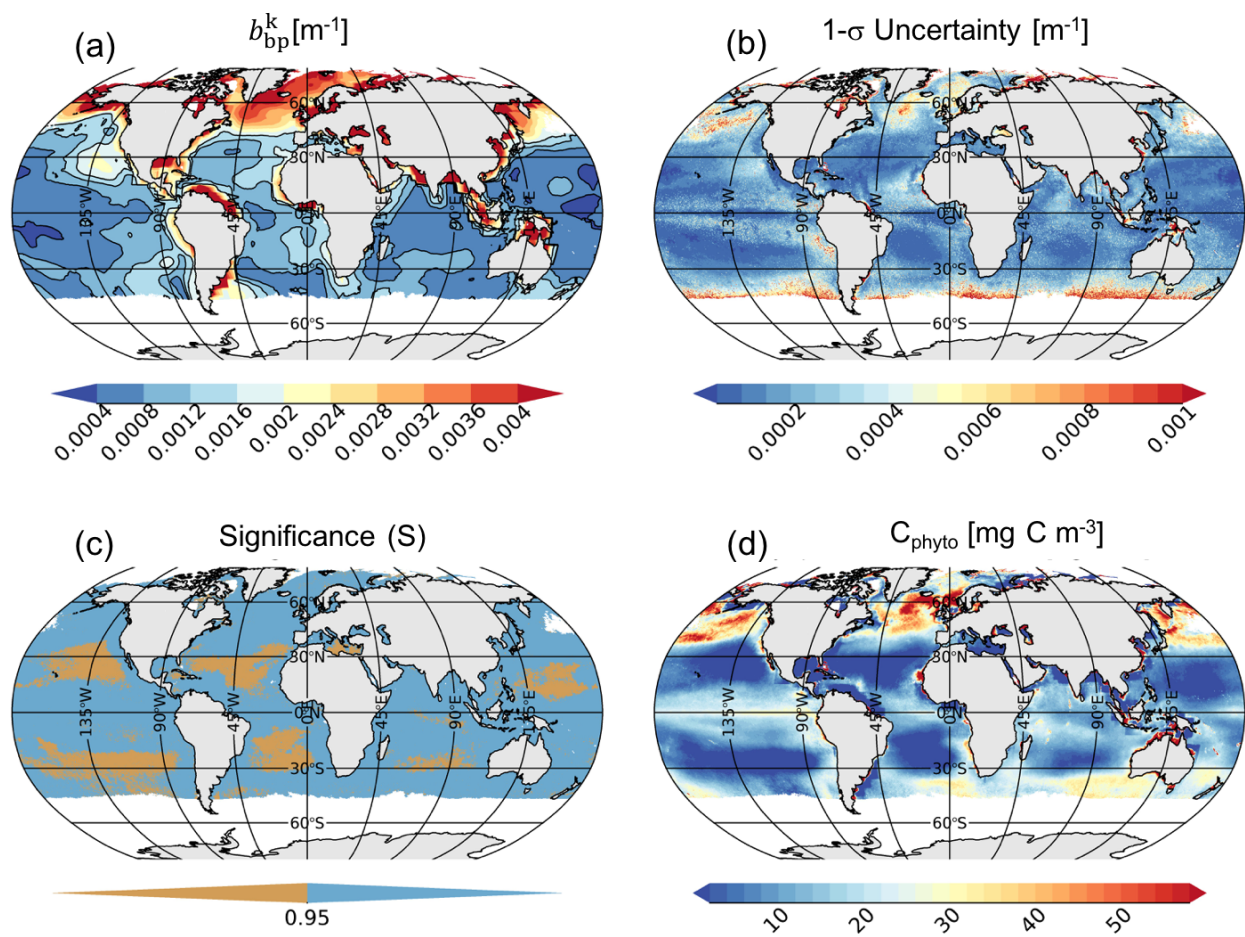


Figure S7. June global mean climatological of b_{bp}^k (a), 1- σ uncertainty (b), significance S (c) and C_{phyto} (d).

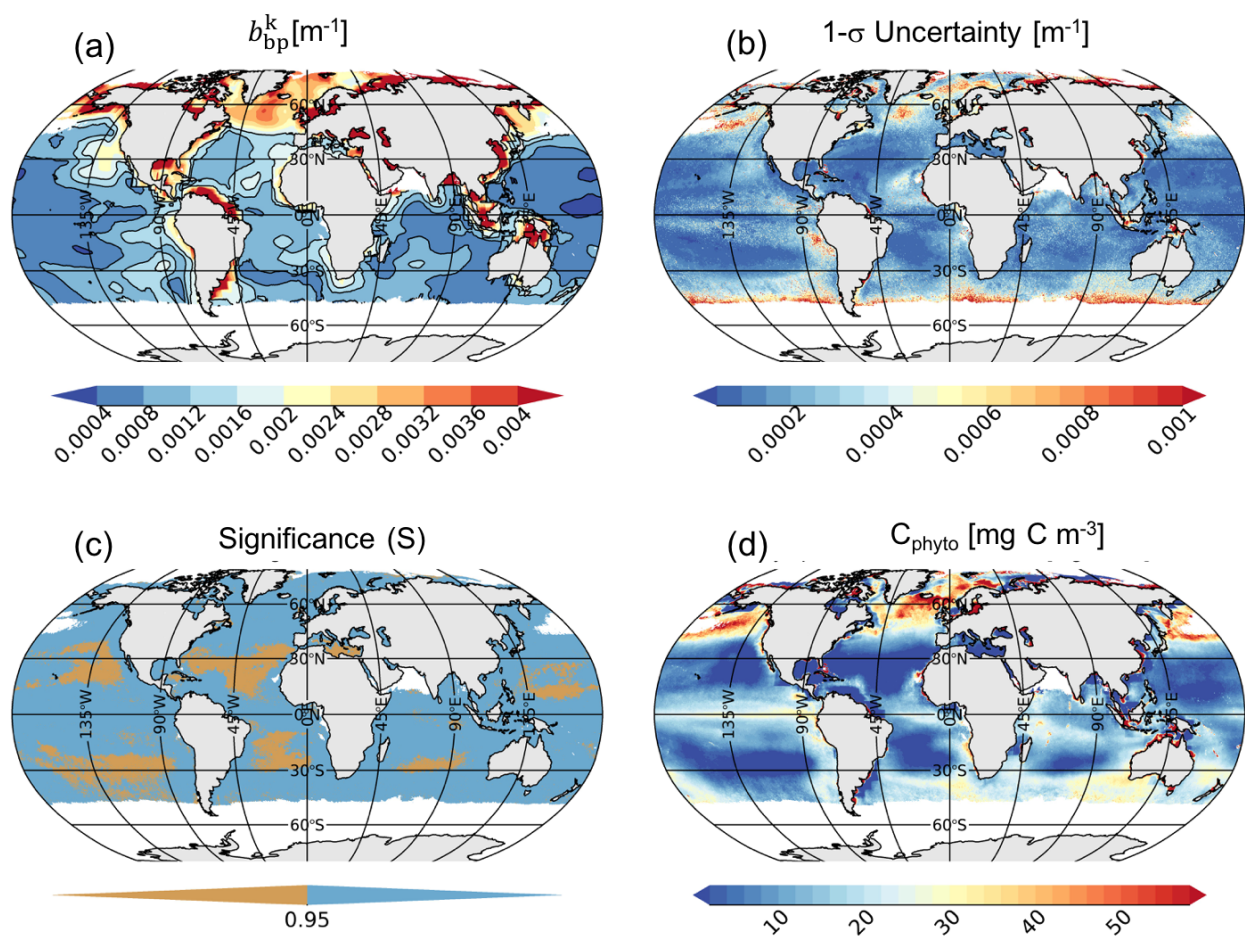


Figure S8. July mean global mean climatological of b_{bp}^k (a), 1- σ uncertainty (b), significance S (c) and C_{phyto} (d).

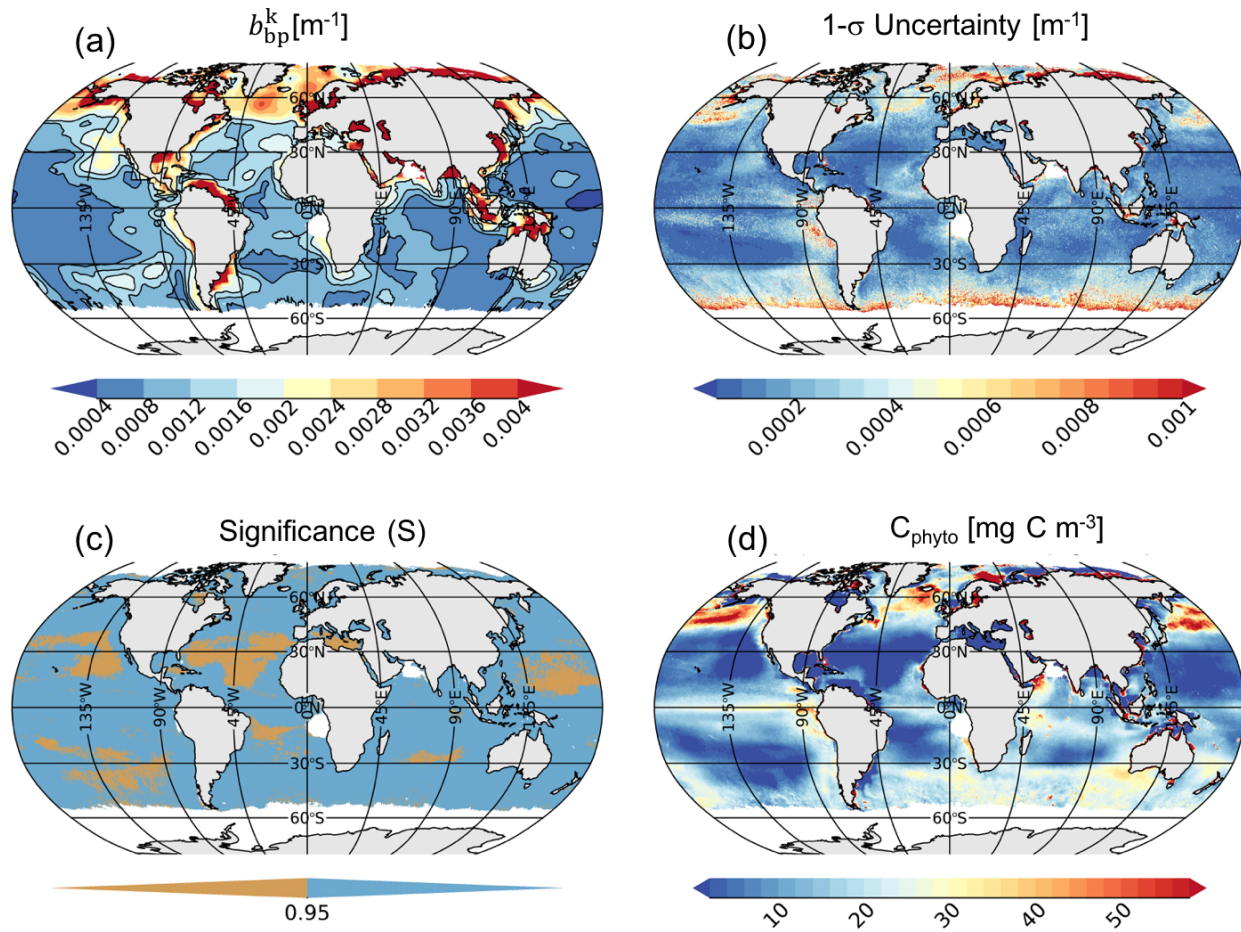


Figure S9. August global mean climatological of b_{bp}^k (a), 1- σ uncertainty (b), significance S (c) and C_{phyto} (d).

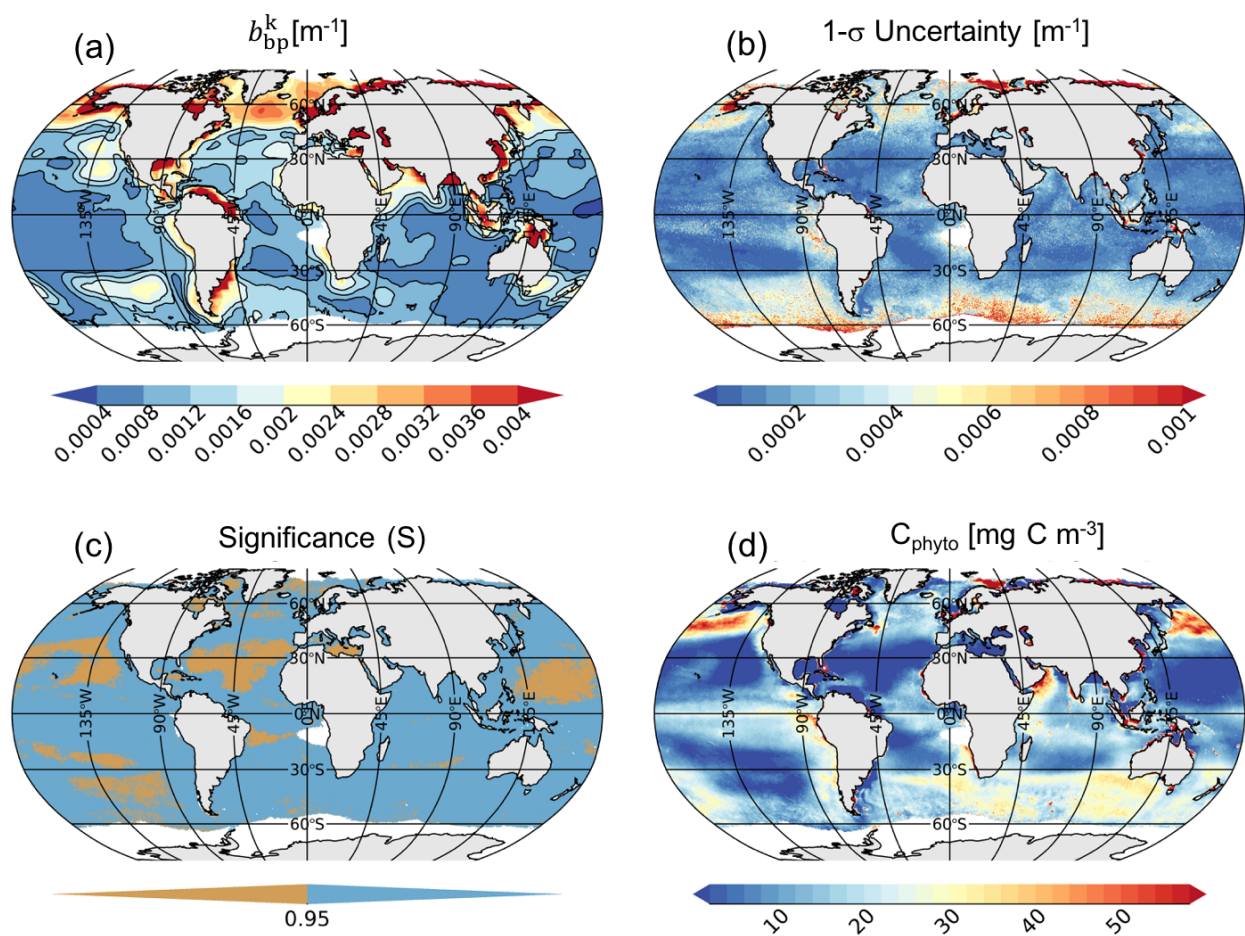


Figure S10. September global mean climatological of b_{bp}^k (a), 1- σ uncertainty (b), significance S (c) and C_{phyto} (d).

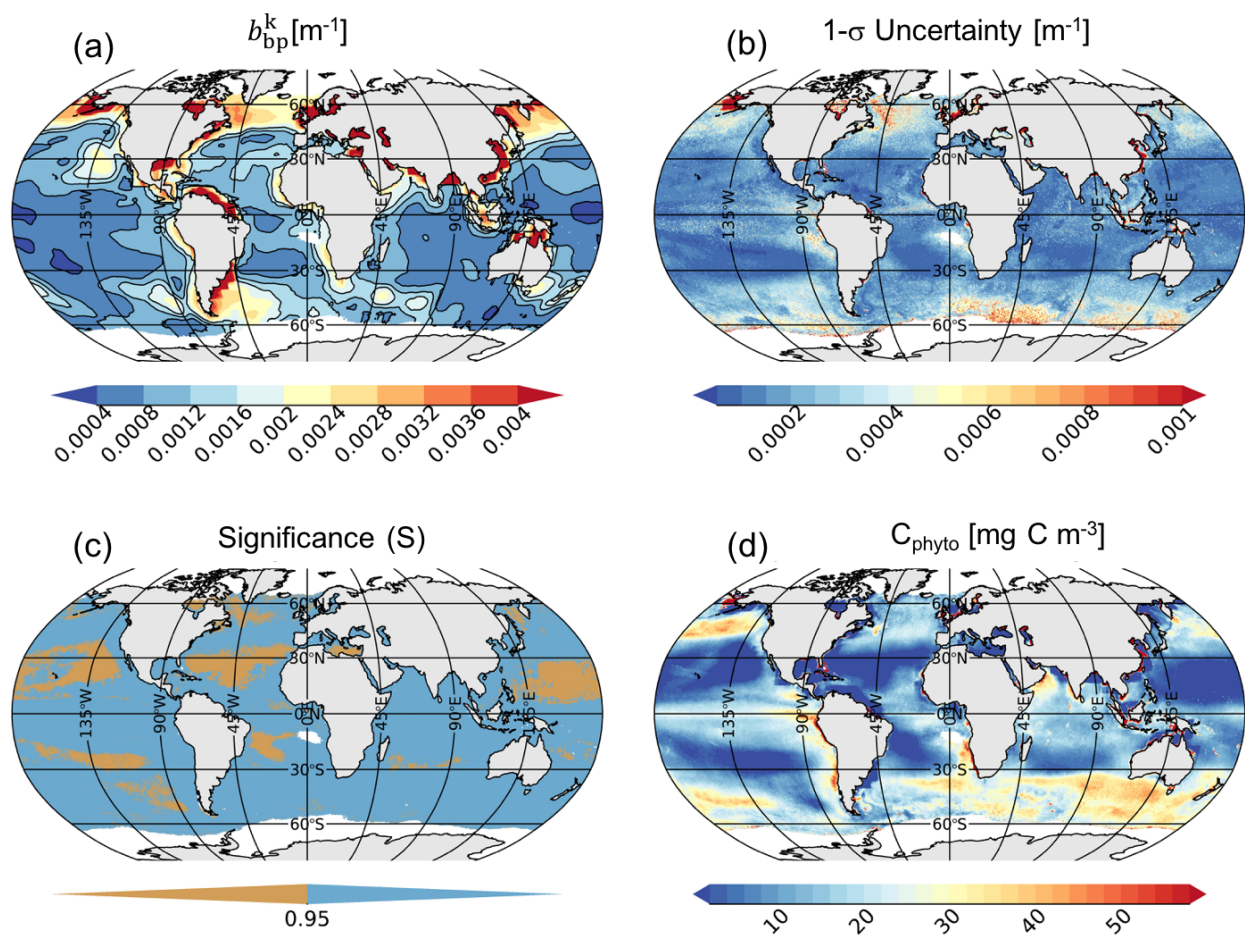


Figure S11. October global mean climatological of b_{bp}^k (a), 1- σ uncertainty (b), significance S (c) and C_{phyto} (d).

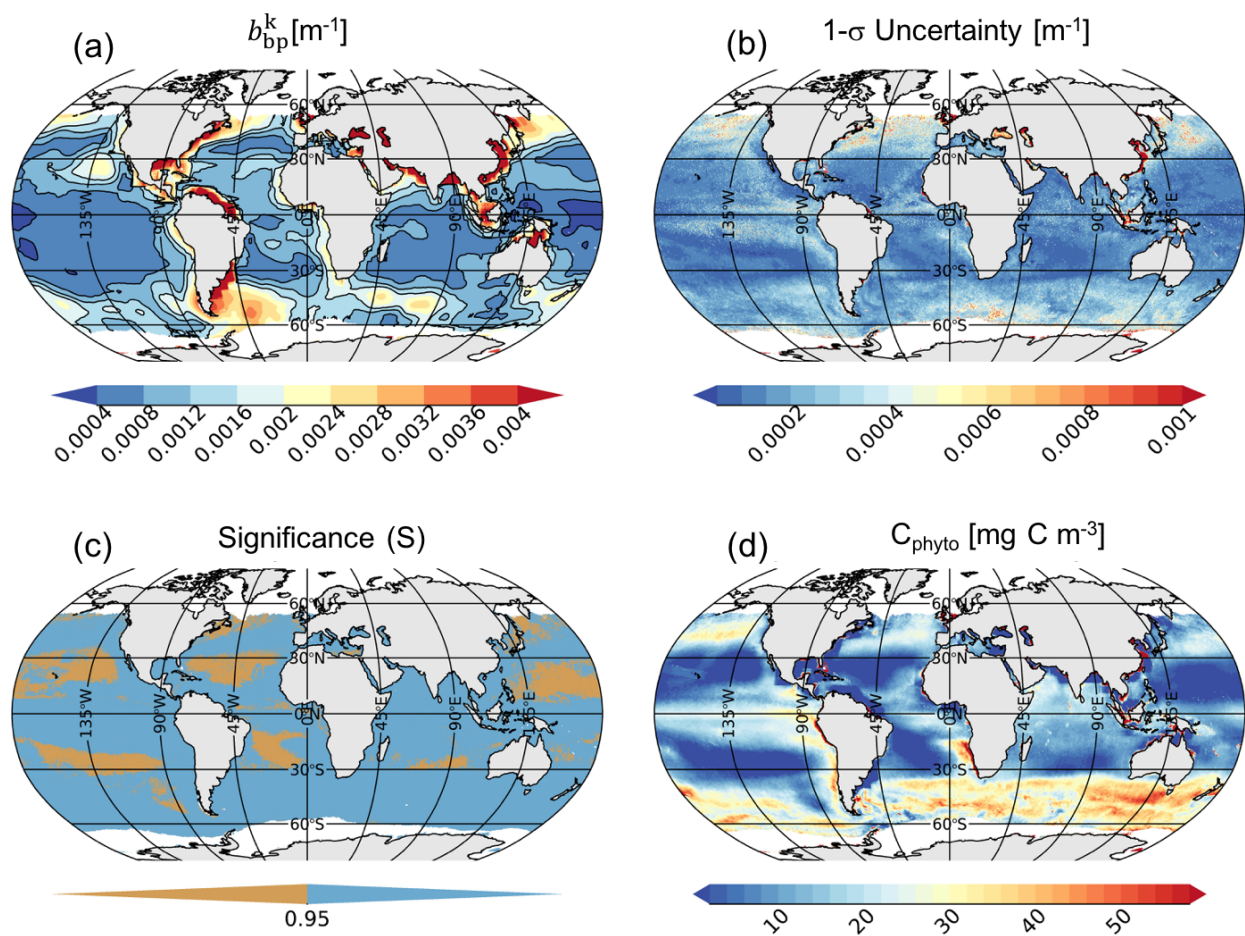


Figure S12. November global mean climatological of b_{bp}^k (a), 1- σ uncertainty (b), significance S (c) and C_{phyto} (d).

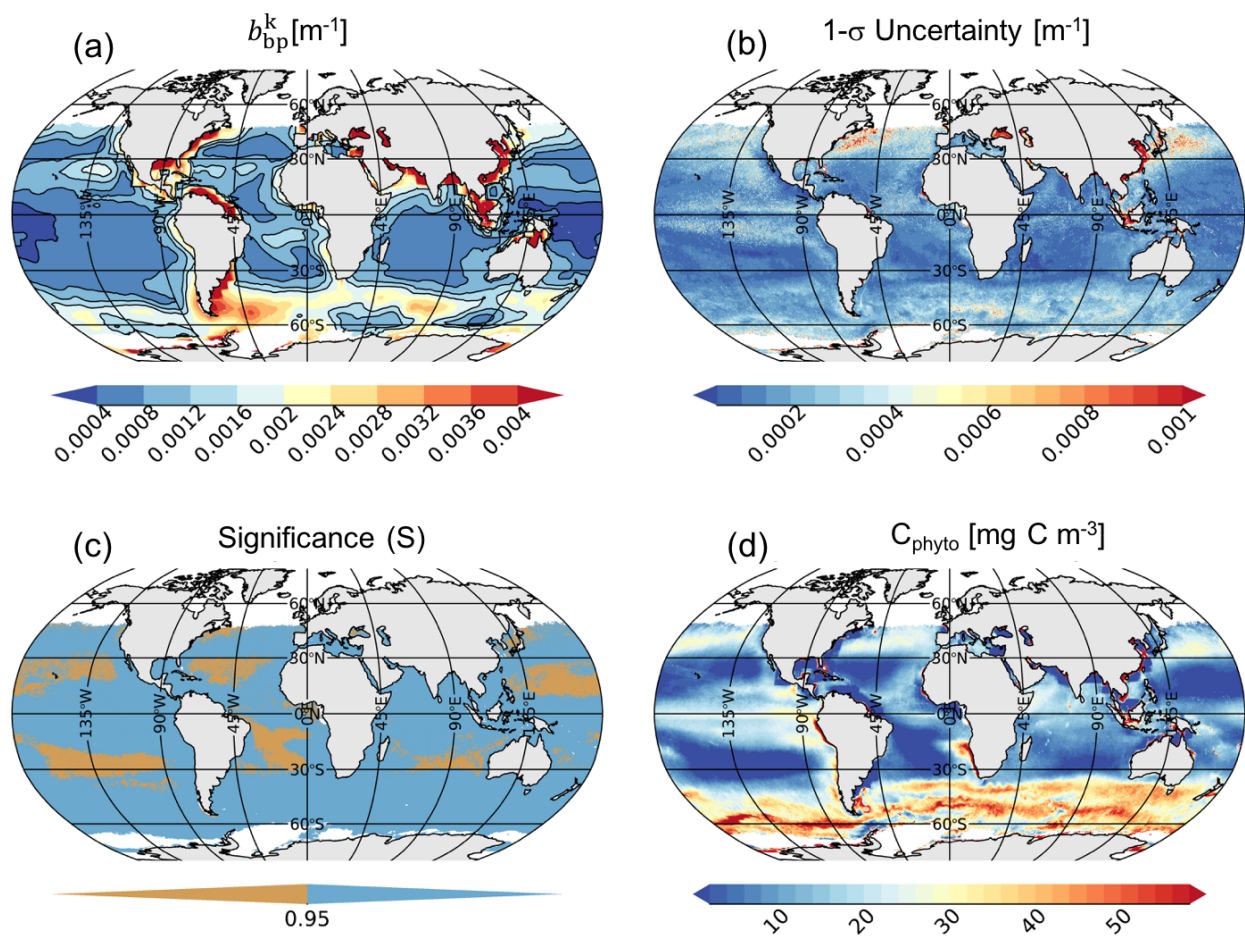


Figure 13. December global mean climatological of b_{bp}^k (a), 1- σ uncertainty (b), significance S (c) and C_{phyto} (d).

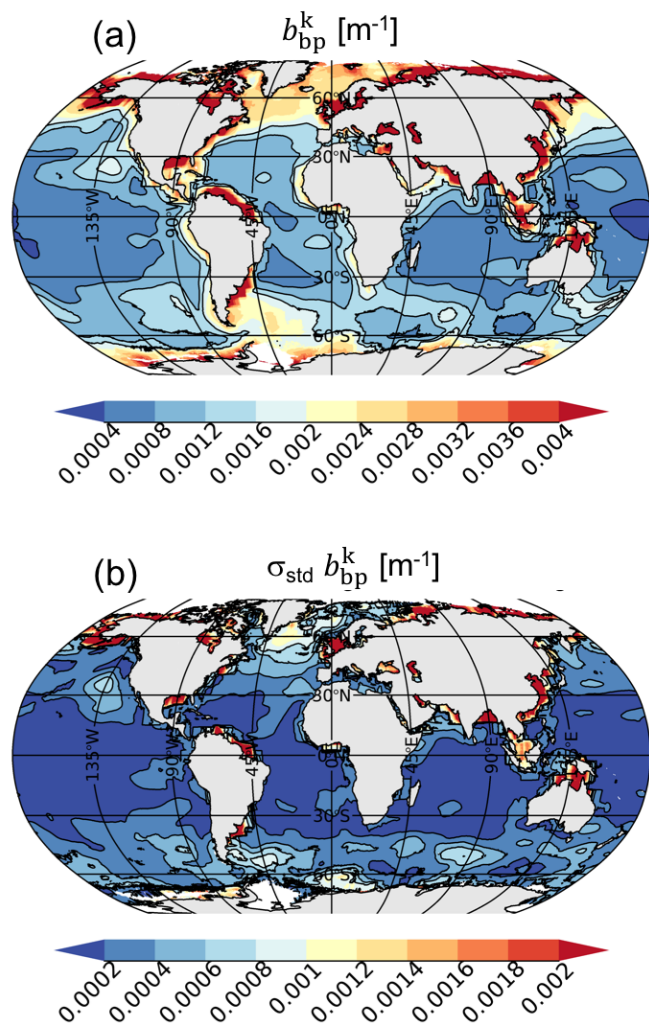


Figure 14. global mean (a) and standard deviation (b) of b_{bp}^k . Note that at high latitudes, the number of satellite observations used for the mean and standard deviation computations are lower than those used at low or mid-latitudes due to the winter darkness.